

Uncertainties in future ecosystem services under land and climate scenarios: The case of erosion in the Alps

Nicolas Elleaume^{a,*}, Bruno Locatelli^b, David Makowski^c, Améline Vallet^{d,e}, Jérôme Poulenard^f, Johan Oszwald^g, Sandra Lavorel^a

^a Laboratoire d'Ecologie Alpine, Université Grenoble Alpes, Université Savoie Mont-Blanc, CNRS, Grenoble, France

^b CIRAD, University of Montpellier, France

^c UMR 518, INRAE, Université Paris-Saclay - AgroParisTech, France

^d Ecologie Systématique Évolution, AgroParisTech, CNRS, Université Paris-Sud, Université Paris-Saclay, Orsay, France

^e CIREN, AgroParisTech, Cirad, CNRS, EHESS, Ecole Des Ponts ParisTech, Université Paris-Saclay, Nogent-Sur-Marne, France

^f EDYTEM, Université Savoie Mont-Blanc, Bourget-du-Lac, France

^g LETG Rennes COSTEL, Université de Rennes 2, France

ARTICLE INFO

Keywords:

Ecosystem service
Uncertainty
Alps
Climate change
Land use and land cover change
RUSLE

ABSTRACT

How ecosystems will provide ecosystem services in the future given uncertain changes in climate and land use is an open question that challenges decision-making on adaptation to climate change. Prospective assessments of ecosystem services should carefully include and communicate the sources of uncertainties that affect the predictions. We used the ecosystem service of soil protection against erosion in the Maurienne Valley (French Alps) as a case study to illustrate how several sources of uncertainties can be integrated into an assessment of future ecosystem service supply. We modeled future erosion rates in the Maurienne Valley for years 2020 and 2085 using the Revised Universal Soil Loss Equation (RUSLE) and six climatic and socioeconomic scenarios. We quantified how the ecosystem service supply will be likely affected by climate and land-use change, separately and jointly. We assessed the effects of different sources of uncertainty on projected erosion rates: scenarios, climate models choice, and methods to parametrize the ecosystem service model. Land-use change increased erosion (+ 3.3 ton.ha⁻¹.yr⁻¹ on average, with significant increases in 81 % of the study site), while climate change contributed to a slight reduction (-0.21 ton.ha⁻¹.yr⁻¹ on average with significant decrease 20 % of the study site). The uncertainty of the ecosystem service model parameterization explained 93 % of the variance in erosion values. Furthermore, uncertainty linked to climate models and future scenarios contributed almost equally to the variability in the direction (positive or negative) of erosion change (41 % and 38 % respectively). The uncertainties surrounding the direction of future changes in ecosystem services come mainly from uncertainties in climate models and future scenarios rather than from uncertainties in the ecosystem service model parameters. Assessing the likelihood of future changes in ecosystem services helps prioritize locations where adaptation solutions are likely to be needed.

1. Introduction

Ecosystems and the services they provide (ecosystem services, ES) are under increasing pressure from global drivers of change, particularly climate change and land use and land cover (LULC) transformations. Climate change directly affects ecosystems by altering temperature, precipitation patterns, and the frequency of extreme weather events, leading to shifts in ecosystem processes and biodiversity loss (Masson-Delmonte et al., 2021). LULC changes, shaped by human activities and socioeconomic dynamics, further compound these pressures

by modifying habitat structures, ecosystem functions, and ES supply (Díaz et al., 2019; Song et al., 2018). While climate and LULC changes often interact to exacerbate ecosystem degradation, LULC changes can also offer opportunities for adaptation. Strategic land management, such as forest restoration or sustainable agricultural practices, has the potential to mitigate the adverse effects of climate change by enhancing ecosystem resilience and maintaining ES supply (Fedele et al., 2018; Lavorel et al., 2020; Pyke and Andelman, 2007). These adaptation strategies, often referred to as ecosystem-based adaptation or nature-based solutions, provide dual benefits: they reduce human

* Corresponding author.

<https://doi.org/10.1016/j.ecolmodel.2025.111041>

Received 31 March 2024; Received in revised form 20 December 2024; Accepted 5 February 2025

Available online 16 February 2025

0304-3800/© 2025 The Authors. Published by Elsevier B.V. This is an open access article under the CC BY-NC-ND license (<http://creativecommons.org/licenses/by-nc-nd/4.0/>).

vulnerability to climate risks while promoting biodiversity conservation and social co-benefits (Albert et al., 2021; Jones et al., 2012).

Designing effective adaptation strategies requires robust knowledge of how ES will respond to future changes in climate and LULC. This knowledge is crucial to anticipate risks, avoid maladaptive decisions, and identify opportunities for sustainable resource management (Chhetri et al., 2019; Lavorel et al., 2019). However, predicting future ES supply is challenging due to the inherent uncertainties associated with global change drivers and the ES modelling process. These uncertainties may arise from the variability in future climate trajectories, socioeconomic development pathways, input data choices and quality, ES model choice, model parametrization and their inherent limitations (Refsgaard et al., 2007). Addressing these uncertainties is essential to provide reliable projections that can inform policy and decision-making.

Because uncertainties arise from many steps in the modeling process, assessing their contributions to the variability of model outputs is recognized as a challenge for the ES modeling and mapping community (Hamel and Bryant, 2017). Current approaches of uncertainty analysis in ES modeling often focus on quantifying the variability associated with input data, such as climate projections, land use scenarios, or socio-economic pathways and their propagation to the model output (Baustert et al., 2018; Refsgaard et al., 2007). Scenario-based modeling, for instance, is commonly used to explore how alternative futures may impact ES supply (Hamel and Bryant, 2017). Similarly, multi-model ensembles are employed to capture the range of possible outcomes from different modeling frameworks, particularly in climate and hydrological studies (van Vliet et al., 2016; Veerkamp et al., 2023; Vetter et al., 2015). While approaches, such as Monte Carlo simulations, geostatistics, difference maps or grid-uncertainty maps, are increasingly used to address uncertainties in modeling, they are still marginally used in the ES assessment community (Hamel and Bryant, 2017; Visser et al., 2006). Furthermore, spatially explicit uncertainty assessments provide critical insights for localized adaptation planning but also remain underutilized (Baustert et al., 2018; Strith et al., 2018; Visser et al., 2006).

This methodological gap underscores the need for comprehensive analysis that incorporate multiple sources of uncertainty while providing actionable, spatially explicit outputs (Visser et al., 2006). Addressing this gap is essential for advancing ES modeling and ensuring its relevance for decision-makers operating under complex and uncertain future conditions. To address the limitations of prospective ES assessments and integrate multiple sources of uncertainty, we adopted the uncertainty framework proposed by Walker et al. (2003), refined by Refsgaard et al. (2007). This framework categorizes uncertainties by their location in the modelling process (e.g., data inputs, model structure), nature (e.g., variability or knowledge gaps), and type (e.g., statistical or scenario-based). Using this framework, we evaluated three sources of uncertainty:

1. Scenario uncertainty: Variability in socioeconomic and emission trajectories.
2. Climate model uncertainty: Differences in projections across multiple climate models.
3. Model parameter uncertainty: Assumptions related to the parametrization of the ES model.

In this study, we focus on soil erosion regulation in the French Alps, a critical regulating service in mountainous regions. Soil erosion contributes to risk reduction and supports productive activities, such as agriculture (Guerra et al., 2016). However, mountain ecosystems, including the French Alps, are particularly sensitive to climate change, as evidenced by shifts in hydrological cycles, vegetation dynamics, and erosion processes (Hock et al., 2019). Steep slopes, diverse plant cover, and varying land use patterns make erosion regulation a highly context-dependent service, influenced by multiple factors, including rainfall and vegetation changes (López-Vicente and Navas, 2010). To

model soil erosion, we used the Revised Universal Soil Loss Equation (RUSLE), a robust and widely applied empirical model that estimates long-term soil loss based on drivers such as rainfall, soil properties, and land cover (Renard, 1997). RUSLE is particularly well-suited for our study due to its adaptability to different contexts, including alpine regions (Aiello et al., 2019; Borrelli et al., 2020; BoSCo et al., 2009; Giannetto et al., 2020; Panagos, Borrelli, Poesen, et al., 2015). This analysis focused on two key RUSLE factors directly influenced by climate change and LULC projections: rainfall erosivity and land cover changes.

Specifically, this study aimed to: (1) estimate current (2020) and future (2085) erosion rates and disentangle the contributions of climate and LULC changes to these differences; (2) map the level of agreement among models and methods regarding the direction and significance of future erosion changes; (3) quantify the contribution of different uncertainty sources to the magnitude and direction of projected changes. By incorporating three sources of uncertainty and using a novel methodology to map agreement on future ES supply, we provide spatially explicit information on likely changes in erosion, improve understanding on the drivers of these changes, assess the contribution of the sources of uncertainty to model outputs, and provide practical guidance on how our probabilistic mapping of future ES supply can inform adaptation planning decisions.

2. Material & methods

2.1. Overall approach

ES modeling commonly relies on data used as proxies to describe ecosystem state (e.g., land use and land cover maps) or earth observation data (e.g., vegetation indices) (Egarter Vigl et al., 2017; Schägner et al., 2013; Strith et al., 2018). Climate variables are also major inputs to the modeling of ES that are sensitive to climate, especially when assessing the effect of future climate change (Lavorel, 2019; Schirpke et al., 2017). To understand how the future drivers of change with their related sources uncertainty can modify the supply of ES in the future, we used multiple scenarios of future change in LULC and climate. To analyze changes in a phenomenon characterized by interannual variability (i.e., erosion and soil protection depends on annual rainfall), we developed a specific method that can apply to any ES with interannual variability.

Our approach relied on a spatially explicit modeling process that estimated ES supply for two time windows (2020 and 2085) at a 0.005 arc degree spatial resolution. Several scenarios of climate change or LULC change were considered, and we developed an original method to compare present and future maps of the ES supply to assess its change over time. For each time window, to account for the interannual variability of climate variables (rainfall in our case), we produced maps of the ES supply for each year of a 30-year period centered in 2020 and 2085. Those 30 maps accounting for interannual variability of rainfall were produced for all combinations of uncertainty sources accounted here (e.g. LULC and climate scenarios, climate models and ES model parametrization methods).

2.2. Study site

We modeled erosion in the Maurienne valley in the French Alps, a 120-km-long alpine valley located on the border with Italy. Its altitude ranges from 289 to 3571 m a.s.l., with a mean altitude of 2034 m a.s.l. It covers 1 976 km² and its center is located at 45°11'N - 6°39'E (Fig. 1). The valley is shaped by the Arc River which flows from the east to the west. The montane climate has a sharp rainfall gradient from the northwest (more humid) to the southeast (drier). Between 1999 and 2019, the average annual rainfall was 1641 mm in Saint-Rémy-de-Maurienne (western part of the valley) and 1142 mm in Aussois (eastern part). Temperatures follow a west-east altitudinal gradient, with milder average temperatures in the west (4.6 °C mean annual temperature in

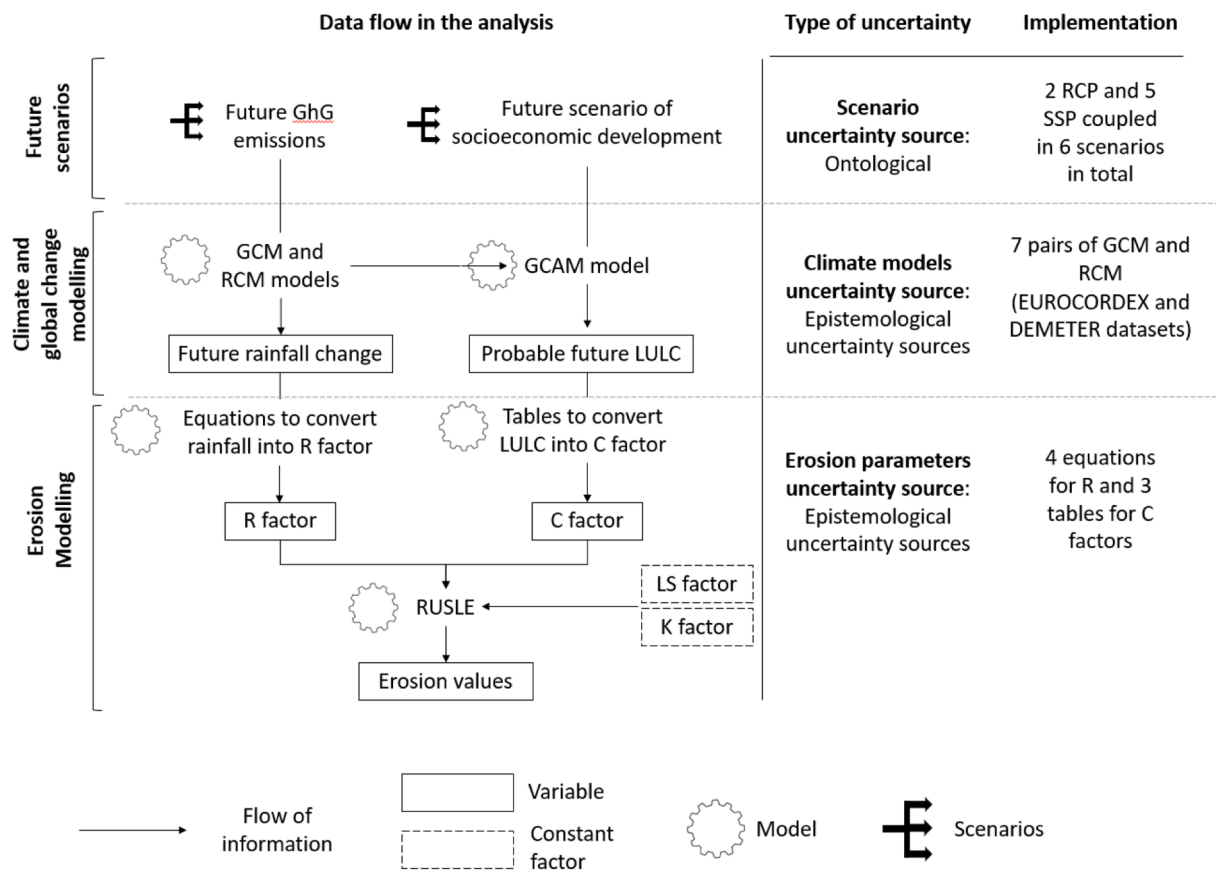


Fig. 1. Data flow for the uncertainty sources assessed in the analysis. Acronyms in the figure stand for: GhG: Greenhouse Gases, RCP: Representative Concentration Pathway, SSP: Shared Socioeconomic Pathway, GCM: Global Circulation Model, RCM: Regional Climate Model, GCAM: Global Change Assessment Model, LULC: Land Use and Land Cover, R factor: Rainfall erosivity factor, C factor: land cover factor, LS: Slope length and steepness factors, K: soil erosivity factor, RUSLE: Revised Universal Soil Loss Equation.

Saint-Rémy-de-Maurienne) and colder average temperatures in the east (0.1 °C mean annual temperature in Aussois). The catchment geology in its far western part is mainly ortho-gneiss or locally schist (low to medium erodibility) followed by a large band of schist, conglomerate, and flysch (high erodibility) extending until the central area of the valley with coal and carbonate type rock (low erodibility); the eastern part of the valley is formed of lustrous shales, i.e. calcareous and detrital sediments, as well as ophiolites (medium to high erodibility).

Land cover comprises a high share of bare soils (36 %), mainly located at high altitude in the eastern part of the valley, while forest covers slopes at low and medium altitudes and grasslands prevail at medium to high altitude (each 26 %). The rest of the landscape is composed of shrubs (5 %), glaciers (2 %) at very altitudes, built-up land (2 %) and water surfaces (1 %) (Fig. 1).

2.3. Erosion model

The RUSLE model was originally developed for U.S. agricultural land management at the parcel scale, but has since undergone multiple developments (Renard, 1997; Wischmeier and Smith, 1978). In particular, remote sensing data and Geographical Information Systems (GIS) have allowed using the RUSLE model at larger scales: from the watershed level to the earth scale (Fu et al., 2005; Kouli et al., 2009; Lu et al., 2004; Panagos et al., 2015; Zhang et al., 2013). The RUSLE model considers six factors affecting soil erosion:

Eq. (1): Revised Universal Soil Loss Equation

$$A = R * C * L * S * K * P \tag{1}$$

Where A is the soil loss estimation in $\text{ton} \cdot \text{ha}^{-1} \cdot \text{yr}^{-1}$, R is the rainfall

erosivity factor (i.e. the erosion power of rainfall) in $\text{MJ} \cdot \text{mm} \cdot \text{ha}^{-1} \cdot \text{h}^{-1} \cdot \text{yr}^{-1}$, K is the soil erodibility factor (i.e., the sensibility of soils to erosion) in $\text{ton} \cdot \text{h} \cdot \text{MJ}^{-1} \cdot \text{mm}^{-1}$, L is the slope length (dimensionless), S is the slope steepness (dimensionless), C is the vegetation cover factor (dimensionless, between 0 and 1), and P is the effect of soil conservation practices (dimensionless, between 0 and 1) (Eq. (1): Revised Universal Soil Loss Equation). In the absence of information on soil conservation practices in the studied area, we used a constant value of one for the P factor (i.e. we ignored its effect on erosion). The factors linked to slope (LS factor) and soil texture (K factor) were also considered constant at our time scale, the Table 2 provides information on the data we used to calculate them, also, a full description of the methods used to estimate those parameters is available in Supplementary Materials D and E.

Rainfall erosivity (the R factor) is usually calculated using the maximal rainfall intensity at a 30 mins temporal resolution (Renard, 1997). As this type of hourly climate data was not available for future projections, we estimated the R factor based on annual rainfall data following Renard (1997). Rainfall erosivity was calculated for two time-periods of 30 years centered in 2020 for the present and 2085 for the future. The annual rainfall data were transformed into rainfall factors used inside the ES model by using 4 different equations accounting for the uncertainty in the model parameterization (see Supplementary material B).

Cover factor (the C factor) were derived from LULC classes using conversion tables with the minimum, mean and maximal values of the ranges indicated by (Panagos et al., 2015) (see Supplementary material C for a description of the conversion tables). Given the probabilistic nature of the LULC data, each erosion calculation used a mean value of the C factor weighted by the probability of each LULC (as each LULC was

associated to a probability and a value of C according to a cover factor table).

2.4. Climate scenarios

Future precipitation was estimated using climate projections derived

from different models that simulate the effects of greenhouse gas (GHG) emissions on climate variables under multiple socio-economic and emission scenarios (Fig. 2).

We selected six future socio-economic scenarios provided by the IPCC. These scenarios are the IPCC Shared Socioeconomic Pathway (O'Neill et al., 2014) and Representative Concentration Pathways (Riahi

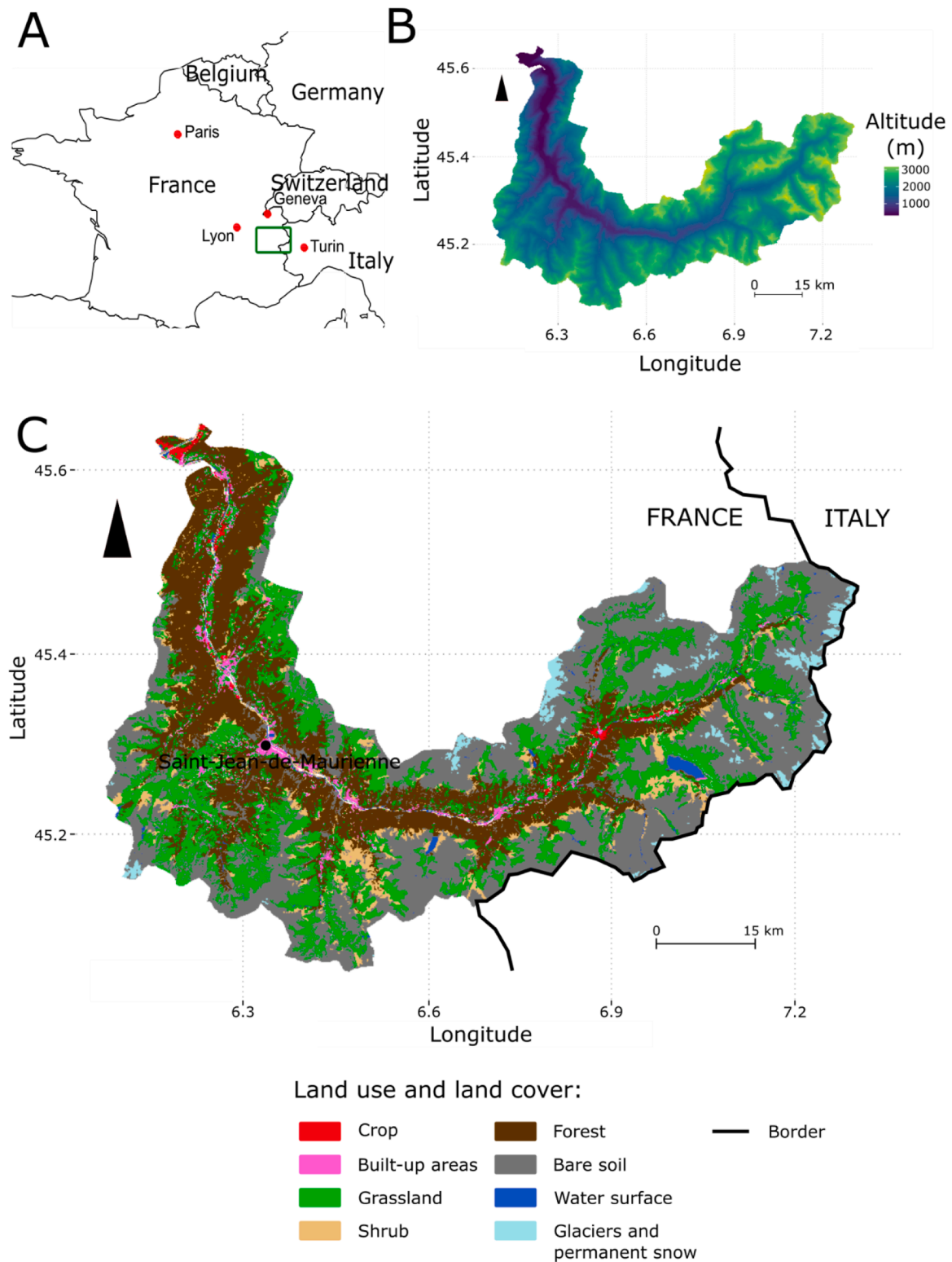


Fig. 2. Study site location, altitude and land use and land cover. A. Location of Maurienne valley. B. Study site digital elevation model. C. Study site land use and land cover in 2016. The detailed land use and land cover dataset is provided by the Data Management Authority from the Savoie department.

et al., 2017; van Vuuren et al., 2011). The Shared Socioeconomic Pathways (SSP) describe possible future trajectories of human societies, including efforts to reduce GHG emissions. The Representative Concentration Pathways (RCP) account for the intensity of radiative forcing induced by atmospheric GHG in the future. Because the SSP and RCP are related, not all combinations of SSP and RCP are evaluated. We selected all combinations of SSP and RCP used in our climate dataset that matched the scenarios used in our LULC datasets, giving 6 couples of SSP-RCP in total (SSP1–5 with RCP4.5 and SSP5 with RCP 8.5). To account for climate model uncertainty, we considered seven different climate models, i.e., combinations of a General Circulation Model (GCM) and a Regional Climate Model (RCM) (Table 1 and Supplementary material A). The climate data for the seven models and the two emissions scenarios (RCP 4.5 and RCP 8.5) was obtained through the ADAMONT method, developed by the EURO—CORDEX project (Verfaillie et al., 2017). The ADAMONT dataset provides climate data specifically for mountain contexts (Verfaillie et al., 2017) (Supplementary material A), structured by altitude slices of 300 m and mountain ranges (seven in our study site).

2.5. LULC scenarios

We used a global land use dataset produced by a Global Change Assessment Model (GCAM) and the Demeter downscaling method (Chen et al., 2020; Chen and Vernon, 2020) (Fig. 2, Tables 1 and 2 and Supplementary Materials A). GCAM are dynamic models simulating economic systems and natural resources under climate change to produce scenarios that include LULC (Calvin et al., 2019). We extracted data for our six SSP-RCP scenarios and our three GCM. The Demeter dataset provides the probability of each pixel to belong to 32 LULC classes, which we aggregated into 6 broad classes (glacier, bare soil, meadows, shrubs, forest, crop, and water surface). We discarded the urban class because we assumed no erosion in urban areas and because many pixels were incorrectly classified as urban (as shown by a comparison with the Sentinel 2 dataset of current LULC). After deleting the urban class, we applied a correction factor to the probabilities to ensure a sum of 1. Finally, we downscaled the dataset to a 150 m spatial resolution by using the disaggregate function with the bilinear method from the raster package (Hijmans et al., 2022) in the R software (R Core Team, 2018 - version 4.0.1).

2.6. Uncertainty assessment

2.6.1. Mapping the likely change in ecosystem service supply despite uncertainty

We first resampled all spatial input data at a spatial resolution of 0.005 arc degree (approximately 220×120 m resolution, with 9537 pixels for the whole study site) with the R software version 4.0.1 (R Core Team, 2018). We then calculated erosion at two time periods (2020 and 2085) for 504 combination of input variables (i.e., combinations of 6 SSP-RCP scenarios, 7 climate models, 4 rainfall erosivity equations, and 3 cover factor tables) (Fig. 2 and Supplementary Material: A, B and C). Erosion was calculated for each year of the two time-periods of 30 years centered in 2020 for the present and 2085 for the future (details in Supplementary Material A-C).

To analyze the significance of ES supply change between 2020 and 2085 considering interannual rainfall variability, and between scenario and model combinations, we performed a Z-test, which compared the 30 values of ES supply in the present with those of the future (normality was verified for 60 % of the pixels across the two 30-year periods using a Shapiro-test). The Z-test was applied for each pixel and each case. We used -1.96 and 1.96 as thresholds for negative or positive significant difference. As we were interested in understanding how climate models and ES model parametrization affected the future direction of change and its likelihood, we calculated to frequencies of significant increase or decrease for each pixel and each of the scenarios of future LULC and

Table 1

Description of the SSP-RCP scenarios used in the study and their effect on the RUSLE model parameters.

Scenarios	Effect on the RUSLE	Name	Description: adapted from Riahi et al. (2017) and van Vuuren et al. (2011)
Representative Concentration Pathway (RCP): Scenarios of future greenhouse gases concentration	Cover factor (C) and Rainfall erosivity factor (R) through climate change and LULC changes.	RCP4.5 (combined with the 5 SSP scenarios) RCP8.5 (combined with SSP5 in this study)	Intermediate scenario of radiative forcing (4.5 W/m ²) in year 2100 Extreme scenario of radiative forcing (8.5 W/m ²) in year 2100
		SSP1	Sustainability (Taking the Green Road). Sustainable path; inclusive development; low material growth and lower resource and energy intensity; low adaptation and mitigation challenges: Middle of the Road. No marked shift from historical patterns; slow progress in achieving sustainable development goals; middle adaptation and mitigation challenges. Regional Rivalry (A Rocky Road). Resurgent nationalism and conflicts; focus on national or regional energy and food security; strong environmental degradation in some regions; high adaptation and mitigation challenges.
Shared Socio-economic Pathways (SSP): Scenarios of socioeconomic change by 2100	Cover factor (C) through LULC		
		SSP2	Inequality (A Road divided). Increasing disparities and inequalities across and within countries; conflict and unrest; focus of environmental policies on local issues around middle- and high-income areas; high adaptation and low mitigation challenges.
		SSP3	Fossil-fueled Development (Taking the Highway). Increasing faith in competitive markets; exploitation of fossil fuel; adoption of resource and energy intensive lifestyles; high mitigation and low adaptation challenges:
		SSP4	
		SSP5	

Table 2
Data sources, nature and description.

Data source	RUSLE factor	Description	Spatial res.	Temp. res.	Reference
Rainfall data	Rainfall erosivity factor (R)	Simulated rainfall data under climate change scenario RCP 4.5 and 8.5 and 7 couples of regional and general circulation model. The dataset used are the products made for mountain context using the ADAMONT downscaling method of the EURO-CORDEX project. Time series are going from 2005 to 2100.	Structured by points accounting for massifs sliced by 300 m of altitude	1-year time steps	http://www.drias-climat.fr/ (Verfaillie et al., 2017)
Land use and land cover data	Cover factor (C)	Simulated future land use and land cover from 2015 to 2090 under 6 future scenarios and 3 GCM. Land use and land cover are distributed originally in 32 classes and each of them are assigned as probabilities on each pixel.	0.05° pixels downscaled to 150 m	5-year time steps	https://data.pnnl.gov/dataset/13192 (Chen and Vernon, 2020)
Digital elevation model	Slope length and steepness (L and S)	Digital elevation model over the study area at 5 m spatial resolution.	5 m	-	https://geoservices.ign.fr/
Soil database	Soil erodibility factor (K)	DonneSol V2 database containing data for multiple soil layers over our study site. Data for organic matter content, clay, silt and sand percentages for the upper layer of soil were used to estimate K factor.	Vector format	-	French National Institute of Agronomic Research (INRAE)

climate change. Pixels were classified into four categories: likely increase (with <10 % of cases of significant decrease and >10 % of significant increase), likely decrease (with <10 % of cases of significant increase and >10 % of significant decrease), likely no change (with <10 % of cases of both significant increase and decrease), and uncertainty (with >10 % of cases of both significant increase and decrease). This method focused on the agreement among cases regarding the future change in the ES supply and thus allowed the rapid identification of locations where future change is likely to be significant (positive or negative), locations where change is unlikely, and locations where change is significant but uncertain because cases disagree on its

direction.

2.6.2. Uncertainty contribution to the magnitude and direction of change

To assess how time affected ES supply in terms of magnitude and the respective contributions of the different uncertainty sources to the ES supply projections, we fitted a linear mixed-effects model using lmer4 package in R and a restricted maximum likelihood method (Bates et al., 2015). The model was fitted on the log-transformed ES values. Time period was set as a fixed effect, while random effects were the SSP-RCP scenario couples, the climate models, and the methods used to parameterize the ES model. The contributions of individual uncertainty sources

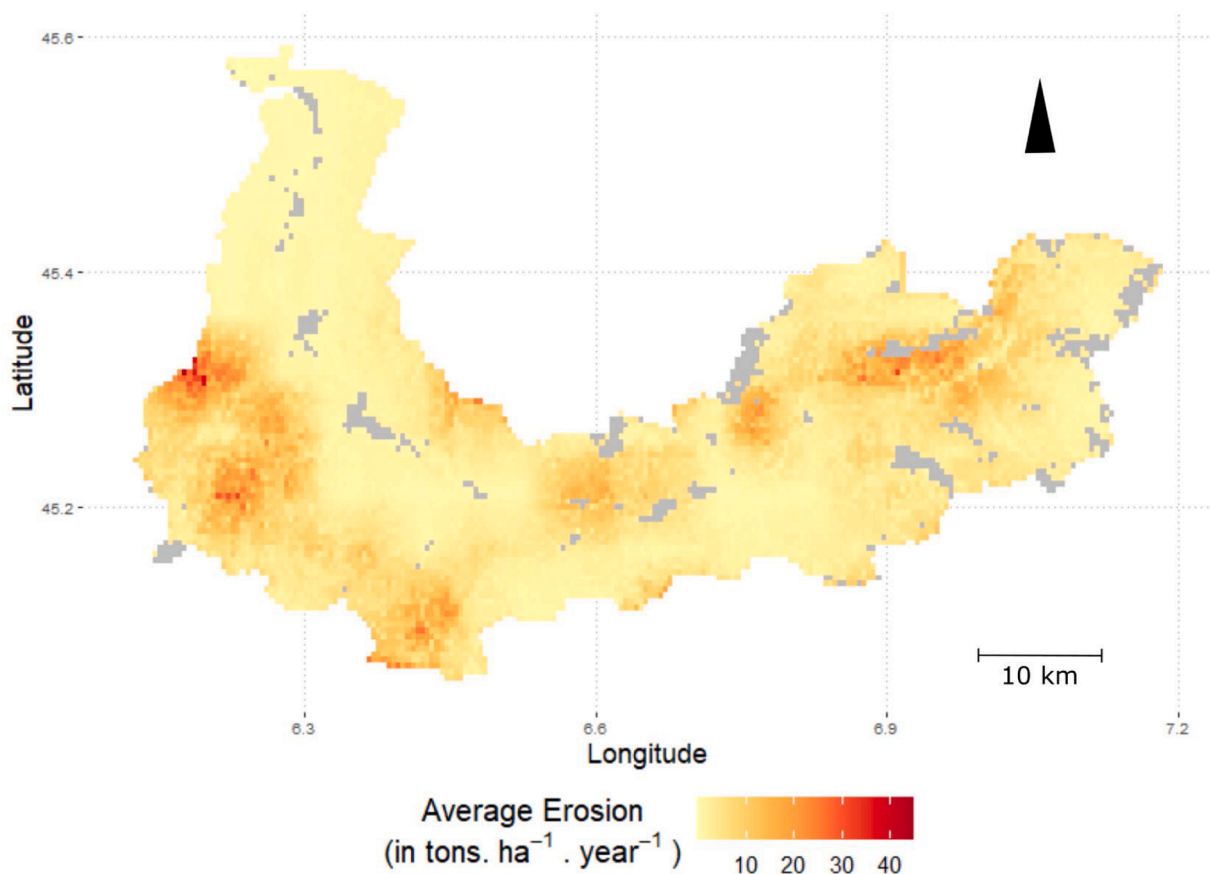


Fig. 3. Soil losses in 2020 in $\text{ton} \cdot \text{ha}^{-1} \cdot \text{yr}^{-1}$. Urban, permanent snow, glaciers, and water were discarded from the analysis and displayed in gray. The climate and LULC datasets were averaged across the six scenarios as they were similar in 2020.

to the overall variability of erosion values were quantified by their respective variance explained.

Finally, to assess how uncertainty sources contributed to the direction of change in ES supply, we transformed the supply differences between 2020 and 2085 into a binary variable indicating positive or negative change in the future. We then fitted a binomial model using the R package lmer4 where all sources of uncertainty were implemented as random effects. This statistical model provides an understanding of how the sources of uncertainty explain the variability of the future direction of ES supply change.

3. Results

3.1. Erosion changes and their drivers

In 2020, erosion rates in the Maurienne Valley ranged from 0 to 46 tons·ha⁻¹·yr⁻¹, with a mean of 4.5 tons·ha⁻¹·yr⁻¹ when averaging over scenarios, climate models and erosion parameterization methods (Fig. 3). Lower values were observed at low and mid-altitudes, primarily in forested areas, while the highest values occurred in steep, high-altitude zones. By 2085, projected changes in erosion ranged from -65 to +134 tons·ha⁻¹·yr⁻¹, with a mean increase of +2.9 tons·ha⁻¹·yr⁻¹ across all combinations of input data. LULC changes alone contributed an average increase of +3.3 tons·ha⁻¹·yr⁻¹, while climate change alone led to a small mean reduction of -0.21 tons·ha⁻¹·yr⁻¹ (Fig. 4). The combined effects of LULC and climate change showed that LULC-driven increases often outweighed climate-driven reductions (Fig. 5).

Changes in erosion resulted from changes in land cover change (C factor) and rainfall erosivity (R factor) in several ways. Regarding land cover, increased cropland areas and decreased forest, shrubland, and grassland led to significant increases in erosion rates (Fig. 6A). The "Regional Rivalry" scenario (SSP3 – RCP 4.5) exhibited the greatest increases, reflecting widespread vegetation loss and cropland expansion. Future changes in the C factor depend mostly on future scenarios and almost not on the climate model (Fig. 6B). Variance analysis showed that scenarios explained 23 % of the variance in absolute changes in the C factor, whereas climate models explained only 0.2 % (Fig. 6B). Regarding rainfall erosivity, climate change led to a mean reduction in rainfall erosivity of 4.6 % across models, with the largest reductions observed under RCP 8.5 on average (Fig. 7). This contributed to localized decreases in erosion but did not offset the increases driven by land use changes. Climate models, rather than scenarios, were the main sources of variability in changes in rainfall erosivity, with 67 % of variance explained by climate models compared with 0.4 % by RCP scenarios. Nevertheless, disparities in the direction and magnitude of

future changes were greatest under RCP 8.5 (with a higher standard deviation of change in the precipitation erosivity factor than under RCP 4.5).

3.2. Likelihood of erosion changes under uncertainty

The likelihood of erosion changes varied spatially across the study site. LULC changes led to significant erosion increases in 81 % of the area across scenarios, while climate-driven decreases were significant in 20 % of the area on average across the six scenarios (Fig. 5).

The sustainability scenario (SSP1 – RCP 4.5) predicted the largest areas of significant erosion reduction (18 %), whereas the "Regional Rivalry" scenario (SSP3 – RCP 4.5) projected the highest proportion of significant increases (93 %). Under the "Fossil-fueled Development" scenario (SSP5 – RCP 8.5), uncertainty in the direction of significant change was most pronounced, with 7 % of the area showing conflicting projections of significant increases or decreases, reflecting the large disagreement among climate models regarding future change in rainfall erosivity under the RCP 8.5 (Fig. 7).

The direction of future changes in erosion due to climate change alone was most uncertain under RCP 8.5 (Fig. 5). Under this scenario, the climate models projected conflicting significant increases or decreases in 16 % of the area (compared to <2 % under other scenarios) due to a large disagreement in the change in rainfall erosivity between climate models under RCP 8.5 (Fig. 7). When considering the combined effect of drivers of change, an overlap of LULC-related increases with CC-related decreases mostly resulted in a significant net increase in erosion due to the strongest positive change induced by LULC change (Fig. 5). Under RCP 8.5, some uncertainties in CC-related changes were propagated to the overall trend by both climate and LULC changes, while others were offset by LULC-induced increases (Fig. 5). In all other scenarios, the addition of the two drivers of change slightly increased the occurrence of areas of uncertain significant change (+3 % uncertain areas on average across the five scenarios associated with RCP 4.5).

3.3. Contribution of uncertainty sources to the magnitude and direction of changes

The three sources of uncertainty tested in our analysis had very different contributions to the overall uncertainty in either the magnitude or the direction of the predicted change. For the magnitude of erosion change, the uncertainty due to erosion model parametrization was the primary contributor to overall uncertainty, accounting for 93 % of the total variance. Climate model uncertainty explained 6 %, while scenario uncertainty contributed only 1 % (Supplementary Materials F).

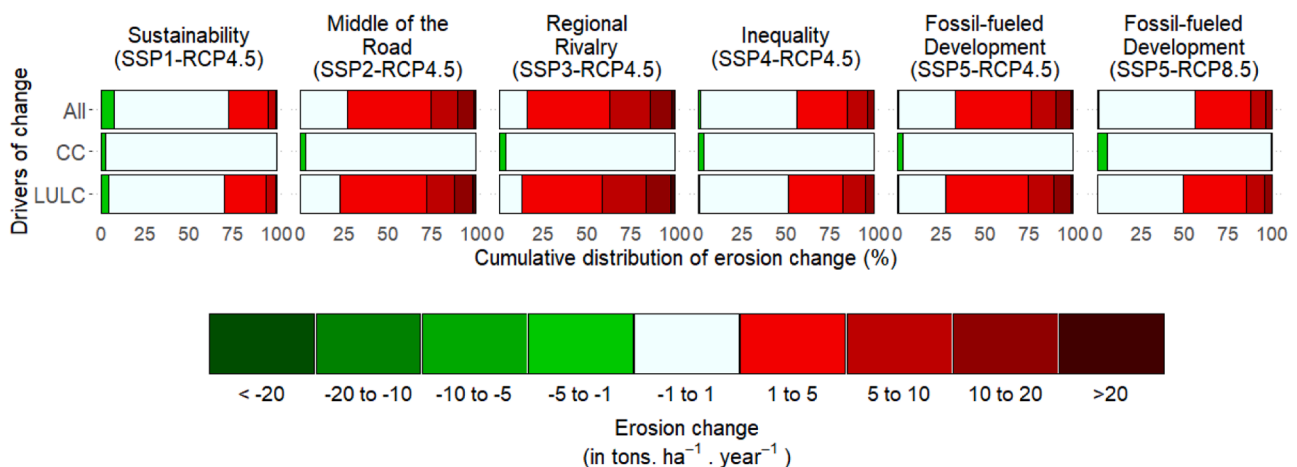


Fig. 4. Cumulative distribution of absolute changes in erosion (ton·ha⁻¹·yr⁻¹) between 2020 and 2085 for different SSP-RCP couples (columns) and drivers of change (rows). Observation unit is the number of pixels over the study site.

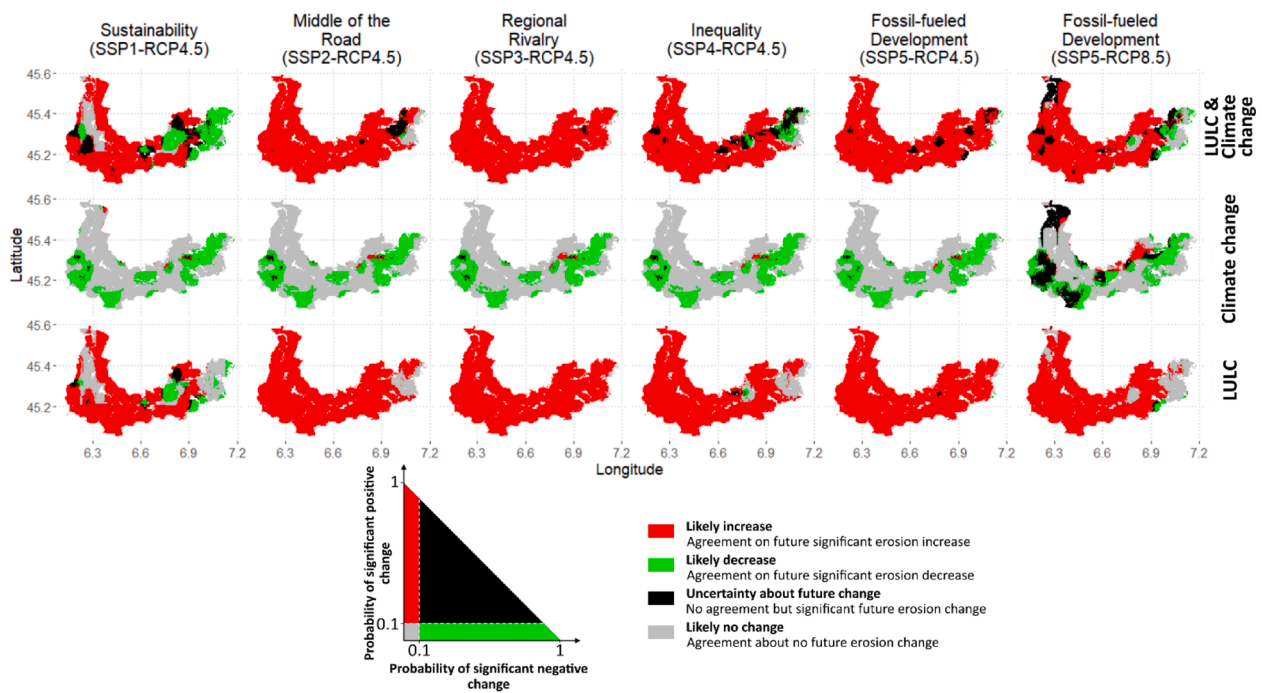


Fig. 5. Likelihood and agreement of future erosion change across climate models and erosion parameters uncertainty sources decomposed future drivers of change and scenarios.

For the direction of erosion change, uncertainty was more evenly distributed across sources. The binomial model of variability in the direction of erosion change showed that the choice of climate models contributed almost as much to the explained variance as scenario uncertainties (41 % and 38 %, respectively), whereas, the erosion parameter uncertainty contributed 21 % of the explained variance (Supplementary Materials F).

4. Discussion

4.1. Projected erosion changes and their drivers in the Maurienne Valley

Our results indicate significant changes in soil erosion across the Maurienne Valley by 2085, with an overall increasing trend primarily driven by LULC changes. Current erosion estimates from our study (4.5 ton·ha⁻¹·yr⁻¹ on average) align closely with Europe-wide findings (Panagos et al., 2015a), showing similar spatial patterns: lower rates in valley floors and higher rates in steep, high-altitude areas. Future projections indicate that, whereas climate change has only a small overall effect on erosion, it influences spatial variability through changes in rainfall erosivity, consistent with previous studies (Panagos et al., 2021). Our findings highlight the dominant role of LULC dynamics in shaping erosion trends, particularly in mountain regions where land management decisions critically influence soil loss.

Under the intermediate RCP 4.5 emissions scenario, our projections show that socioeconomic pathways drive divergent outcomes, with SSP1 (sustainability) resulting in the smallest increases in erosion, while alternative pathways project substantial increases due to intensified land use pressures. Overall, LULC changes emerge as the dominant driver of erosion increases, largely exceeding the modest decreases induced by climate change. This is consistent with previous research, which highlights the critical role of LULC dynamics as both a driver of increased erosion risk and a potential adaptation strategy to mitigate climate-induced impacts (Gianinetto et al., 2020; Mullan et al., 2012). Specifically, future cropland expansion and losses of natural vegetation are the primary contributors to increased erosion rates, as documented in studies by Vanwalleghe et al. (2017) and Borrelli et al. (2020).

Our analysis highlights the variability introduced by climate model outputs, particularly under the high-emissions SSP5 – RCP 8.5 scenario, where rainfall projections varied significantly across climate models, leading to uncertain predictions in 16 % of the study area. While changes in rainfall erosivity are highly sensitive to the selected climate model, land cover changes are more strongly influenced by socioeconomic scenarios and less affected the choice of climate model. This decoupling underscores the importance of integrating both LULC scenarios and climate models to improve the reliability of ES projections.

4.2. Uncertainty assessment

Our analysis reveals that different sources of uncertainty have distinct impacts on the projections of future erosion. The uncertainty in model parameterization, particularly in the C and R factors of the RUSLE model, is the dominant contributor to variability in the magnitude of erosion estimates. This finding aligns with previous studies that highlight the sensitivity of erosion models to land cover parameterization, as the choice of conversion tables or calculation methods can lead to substantially different erosion rates (Carr et al., 2020; Estrada-Carmona et al., 2017).

Conversely, uncertainties in direction of future significant changes in erosion come primarily from uncertainties linked to climate models and socioeconomic scenarios. Climate models exhibit substantial variability in their projections of rainfall patterns, especially under high-emission scenarios like SSP5 – RCP 8.5. This variability leads to inconsistencies in whether future erosion will increase or decrease across certain areas. Similarly, the inherent unpredictability of future socioeconomic pathways (ontological uncertainty) further contributes to variability in the directional trends of erosion change (Refsgaard et al., 2007; Walker et al., 2003). These findings emphasize the critical need to consider multiple climate models and scenarios in ES impact assessments to adequately capture the range of potential outcomes (Sørland et al., 2018).

By analyzing the contributions of these uncertainty sources, our study highlights a crucial distinction: the variability in erosion magnitudes is driven by epistemic uncertainties (knowledge gaps) in ES model

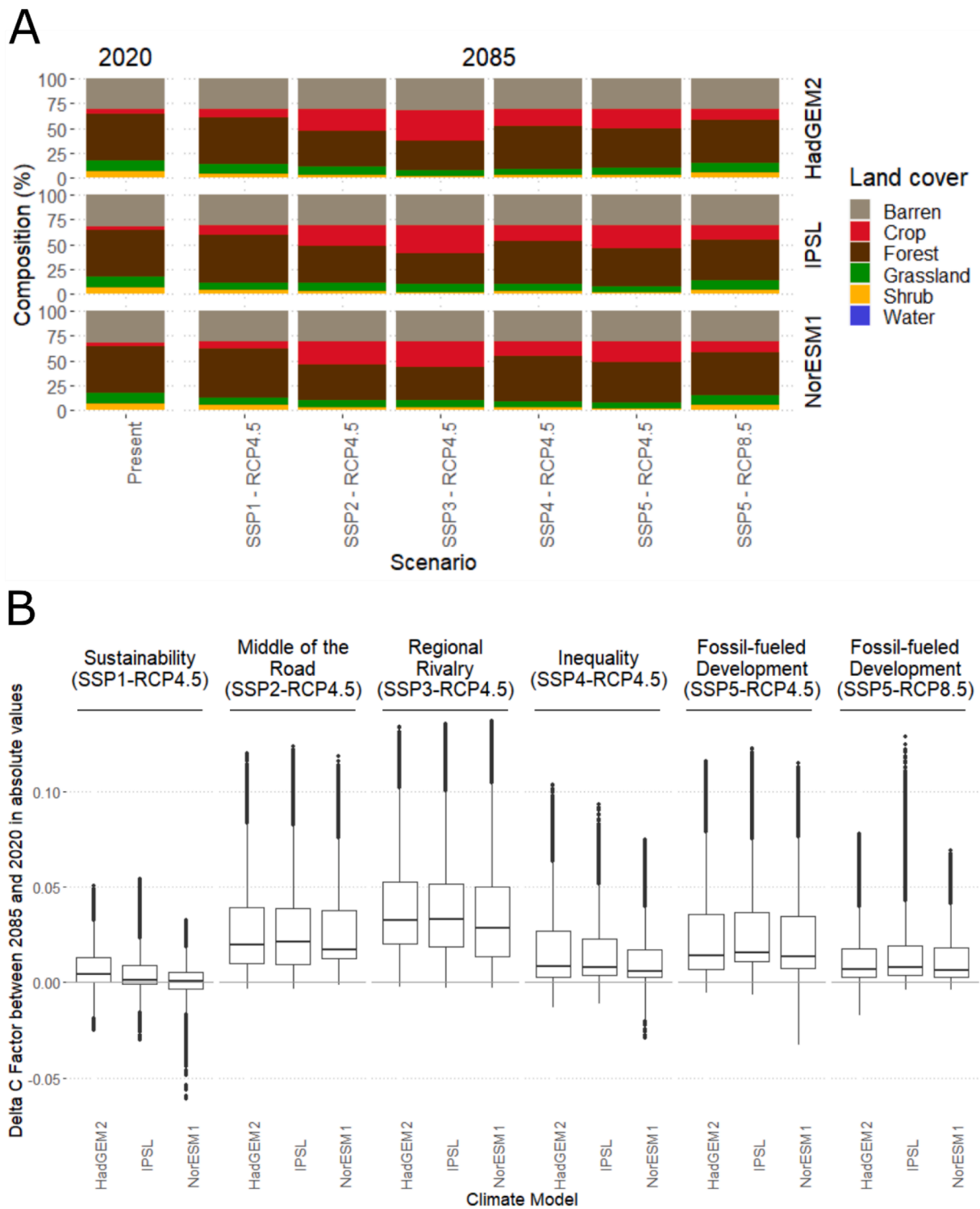


Fig. 6. LULC changes and consequences for C-factor across future scenarios. A: Land use and land cover composition in the study site across the two time periods, the 6 scenarios and the 3 global circulation models. B: C factor absolute difference between 2020 and 2085 by future scenarios and choice of climate models. The boxplot is represented using interquartile range and median while whiskers correspond to 1.5 interquartile range.

parameterization, while the variability in erosion direction is shaped by a combination of epistemic and ontological uncertainties (future unpredictability). This differentiation underscores the importance of tailoring uncertainty management strategies to specific research or policy questions. For instance, efforts to refine predictions of erosion magnitude should focus on improving the accuracy of model parameterization, such as better characterizing C and R factor inputs.

Meanwhile, assessments that aim to identify the likelihood of directional changes should prioritize the integration of diverse climate models and scenarios to capture the range of plausible futures.

Representing diverse uncertainties in a spatially explicit manner is essential for understanding their implications, improving ES modeling, and effectively communicating the uncertainty of model outputs. As Visser (2006) emphasizes, uncertainty mapping should move beyond

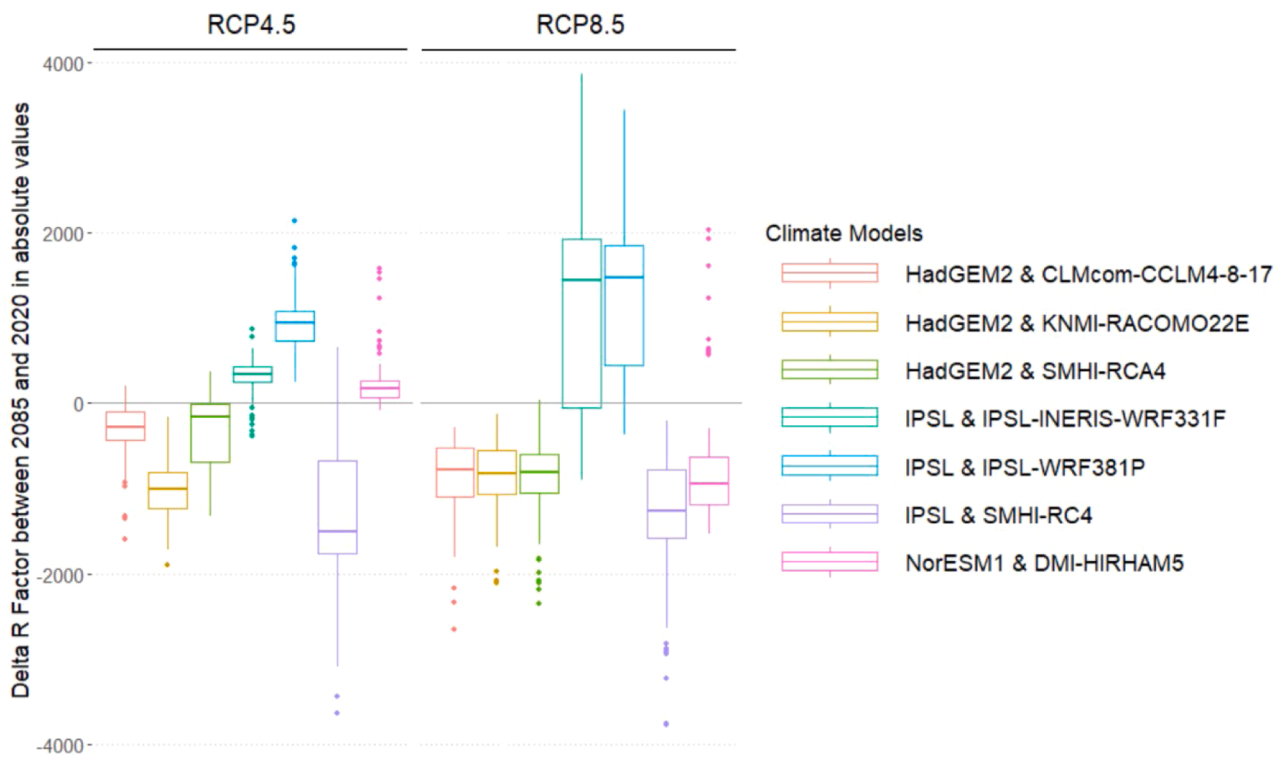


Fig. 7. R factor absolute difference between 2020 and 2085 by future scenarios and choice of climate models. The boxplot is represented using interquartile range and median while whiskers correspond to 1.5 interquartile range.

merely acknowledging variability to making it actionable by distinguishing areas with robust predictions from those with high ambiguity. However, traditional approaches rarely integrate multiple sources of uncertainty into a coherent spatial framework, limiting their potential utility (Hamel and Bryant, 2017). Our approach addresses these challenges by developing a probabilistic mapping framework that includes uncertainties from climate models, LULC scenarios, and model parameterization. By mapping the agreement among these sources regarding the significance and direction of erosion change, we provide a novel visualization that highlights both areas of high predictive confidence and regions of high uncertainty.

4.3. Adaptation to climate change in a context of uncertainty

Our analysis provides actionable insights for guiding adaptation strategies by identifying locations where erosion risks are significant across future scenarios. By integrating multiple sources of uncertainty into probabilistic erosion mapping, we highlight areas of high confidence for erosion increases, as well as regions where uncertainty about the direction of change persists. This spatially explicit approach is particularly valuable for prioritizing adaptation measures and designing targeted interventions to mitigate future erosion risks in an uncertain context (Siders and Pierce, 2021; Visser et al., 2006).

By assessing the likelihood of erosion changes across future scenarios, we can identify key locations of interest for adaptation, where significant increases in erosion consistently appear. The inclusion of two drivers of change (climate change and LULC transitions due to socio-economic changes) enables differentiating adaptation options, as LULC management can reduce future local impacts of climate change (Costanza and Terando, 2019; Duguma et al., 2014; Pyke and Andelman, 2007).

Where LULC transitions from natural areas to crops are the dominant driver of future increased erosion, adaptation efforts could focus on preventing vegetation degradation, such as regulating livestock stocking rates to avoid overgrazing, limiting conversion of grassland to cropland,

or promoting landscape encroachment by abandoning agriculture on the least valuable grasslands (Rey, 2021). Agricultural practices play a crucial role in shaping future erosion risks, particularly through the P factor in the RUSLE model, which accounts for soil conservation techniques and was not integrated in this study. Practices such as reduced or no-tillage and cropland terracing have proven effective in mitigating soil loss (Panagos et al., 2015). In our study area, remnants of early 20th-century agricultural terraces remain visible in the landscape. These terraces, if restored, could act as natural barriers to erosion while enhancing water retention and soil stability. Future research could explore how such measures influence erosion by analyzing how the P factor implementation modify the likely erosion change, offering a pathway for testing candidate adaptation solutions. In contrast, where climate change is the main driver of future erosion change, investing in sustainable agricultural practices, nature-based solutions and ecological engineering to stabilize soils can mitigate impacts (Kumar et al., 2021; Soini et al., 2023). In locations where the direction of future erosion change remains uncertain, no-regret strategies can be prioritized (Heltberg et al., 2009). For example, passive restoration of low-value agricultural lands combined with long-term monitoring could improve erosion mitigation while generating co-benefits for biodiversity and ES (Egarter Vigl et al., 2017). Our probabilistic approach allows for these adaptation strategies to be implemented in areas where confidence in the future ES change is the highest, ensuring adaptation efforts remain effective even under unpredictable future conditions.

In this regard, an innovative but still unexplored feature of our approach lies in its potential to adapt detection thresholds for significant erosion changes to better support decision-making. In our results, thresholds were set at 10 %, but adjusting these thresholds could help refine adaptation priorities. For example, raising thresholds would highlight only the locations experiencing the most certain changes, thereby identifying areas requiring immediate and high-priority adaptation solutions. Conversely, lower thresholds reveal regions with moderate but widespread risks, useful for identifying broader-scale interventions. This feature could make our probabilistic framework

particularly well-suited for tailoring adaptation strategies to the specific needs and resources of local actors.

Our approach demonstrates the potential utility of probabilistic mapping for prioritizing adaptation solutions based on the likely magnitude and direction of change in ES supply, even with uncertain information about the future (Dessai and Hulme, 2004). As climate, socioeconomic trajectories, and adaptation outcomes evolve, this framework can be iteratively refined. By engaging local stakeholders, scientists and decision-makers can co-produce robust adaptation pathways that address local priorities while remaining flexible to emerging data and shifting conditions (Lavorel et al., 2019).

4.4. Limitations

The RUSLE model's C factor, which represents land cover management, is highly sensitive to the choice of conversion tables and methodologies. The variability in these values across different tables contributes significantly to uncertainty in erosion projections. Our study used only one conversion table and examined its minimum, average, and maximum values, but this was insufficient to fully capture the range of possible outcomes. Disagreements in the literature over C values for bare soils (from 0 to 1) highlight the difficulty in accurately characterizing high-altitude land uses, which are critical for understanding erosion dynamics in mountainous regions. Our choice of a C-factor value of 0 for bare soils, following Panagos et al. (2015) led to null erosion values in these areas. Bare soils are mainly located at very high altitude where rainfall and erosivity are also the highest which suggest that we might have underestimated the global erosion rates over the study site (for a detailed analysis of the effect of C factor value in bare soil see Supplementary material G). Better distinguishing between bare rock and bare soil areas in the LULC dataset would help mitigate these methodological biases.

The estimation of rainfall erosivity in our study relied on annual rainfall as a proxy, rather than the modified Fournier index typically used in the RUSLE to assess rainfall erosivity (R factor) over short time scales (e.g., half-hourly resolution) (Renard, 1997; Renard and Freimund, 1994). This approach does not account for extreme rainfall events at fine temporal resolution, which are critical for understanding peak erosion risks (Panagos et al., 2015). The omission of such events restricts our understanding of variability in erosion rates, particularly under scenarios where intense rainfall episodes are projected to become more frequent due to climate change (Calanca, 2007). This limitation underscores the need for a more detailed temporal resolution in rainfall modeling to adequately assess erosion risks.

The use of the GCAM-Demeter LU dataset for LULC projections introduces limitations related to its resolution and scope (Chen et al., 2020). This dataset provides a globally consistent framework but lacks the specificity needed for high-resolution, alpine regions. The coarse resolution prevents the accurate representation of local land use dynamics such as high-altitude greening, tree-line shifts, and grassland encroachment, which can significantly affect erosion patterns (Carlson et al., 2017; Egarter Vigl et al., 2017). As a result, this dataset may: 1) overestimate cropland expansion and vegetation loss, 2) poorly capture the fine dynamics of high-altitude revegetation and tree-line shifts, and 3) ignore the reduction in snow cover that should lead to more erosion in winter, all of which can lead to discrepancies in erosion projections, especially in high elevation areas. Reproducing our analysis with another LULC projection dataset more tailored to the specific Alpine context as well as working on the seasonality of the erosion process are two potential opportunities for improving our model outputs.

Our study focused on integrating specific sources of uncertainty, such as climate models, LULC scenarios, and model parameterization. However, it did not fully account for many other uncertainty sources, such as the uncertainties that are embedded in the datasets used as input data in our modelling process, using other input datasets, spatial and temporal resolution (for climate) of input data, other RUSLE model

parameterization, or the choice of erosion model itself to name a few (Carr et al., 2020; Estrada-Carmona et al., 2017; Walker et al., 2003; Wang et al., 2018). Although it is never possible to include all sources of uncertainty, the integration and analysis of each of these other sources represents a challenge and a new perspective for improving the quantification of uncertainty in predictive ES models (Hamel and Bryant, 2017; Refsgaard et al., 2007).

5. Conclusions

This study provides a comprehensive analysis of future erosion in the Maurienne Valley, highlighting the dominant role of LULC changes in driving significant increases in erosion rates by 2085. While climate change generally decreases erosion through reduced rainfall, its effects are overshadowed by the impacts of projected cropland expansion and vegetation loss, emphasizing the critical need for sustainable land management practices. By integrating multiple sources of uncertainty (including model parameterization, climate models, and socioeconomic scenarios), our probabilistic framework allowed us to map the likelihood of erosion changes, distinguishing areas of high predictive confidence from regions of uncertainty. This distinction revealed that uncertainty in model parameterization primarily affects the magnitude of changes, while uncertainties in climate models and scenarios drive variability in the direction of change. In practice, decision-makers should prioritize interventions in areas where LULC-driven erosion increases are most likely, while employing no-regret strategies, such as revegetation and soil conservation, in regions of where erosion change is highly uncertain. Additionally, adaptive monitoring in areas of high uncertainty can help refine predictions as new data emerge. Future research should aim to validate erosion models with empirical data, test a wider range of inputs data (socioeconomic scenarios and climate models), include other uncertainty sources and further develop probabilistic mapping approaches to better support decision-making in complex and uncertain contexts. This study demonstrates how probabilistic assessments can improve our understanding of likely future changes in ES in a uncertain context, providing insights into ES management research and practice for adaptation to global change.

CRedit authorship contribution statement

Nicolas Elleaume: Writing – review & editing, Writing – original draft, Visualization, Validation, Software, Methodology, Investigation, Formal analysis, Data curation, Conceptualization. **Bruno Locatelli:** Writing – review & editing, Supervision, Software, Project administration, Methodology, Funding acquisition, Formal analysis, Conceptualization. **David Makowski:** Writing – review & editing. **Améline Vallet:** Writing – review & editing. **Jérôme Poulenard:** Writing – review & editing. **Johan Oszwald:** Supervision, Project administration, Funding acquisition. **Sandra Lavorel:** Writing – review & editing, Supervision, Project administration, Funding acquisition, Formal analysis, Conceptualization.

Declaration of competing interest

The authors declare that they have no known competing financial interests or personal relationships that could have appeared to influence the work reported in this paper.

Supplementary materials

Supplementary material associated with this article can be found, in the online version, at [doi:10.1016/j.ecolmodel.2025.111041](https://doi.org/10.1016/j.ecolmodel.2025.111041).

Data availability

Data will be made available on request.

References

- Aiello, M., Gianinetto, M., Vezzoli, R., Nodari, F.R., Polinelli, F., Frassy, F., Rulli, M.C., Ravazzani, G., Corbari, C., Soncini, A., 2019. Modelling soil erosion in the Alps with dynamic RUSLE-like model and satellite observations. *Trends Earth Obs.* 94–97. <https://doi.org/10.1080/22797254.2019.1669491>.
- Albert, C., Brillinger, M., Guerrero, P., Gottwald, S., Henze, J., Schmidt, S., Ott, E., Schröter, B., 2021. Planning nature-based solutions: principles, steps, and insights. *Ambio* 50 (8), 1446–1461. <https://doi.org/10.1007/s13280-020-01365-1>.
- Bates, D., Mächler, M., Bolker, B., Walker, S., 2015. Fitting linear mixed-effects models using *lme4*. *J. Stat. Softw.* 67 (1). <https://doi.org/10.18637/jss.v067.i01>.
- Baustert, P., Othoniel, B., Rugani, B., Leopold, U., 2018. Uncertainty analysis in integrated environmental models for ecosystem service assessments: frameworks, challenges and gaps. *Ecosyst. Serv.* 33, 110–123. <https://doi.org/10.1016/j.ecoser.2018.08.007>.
- Borrelli, P., Robinson, D.A., Panagos, P., Lugato, E., Yang, J.E., Alewell, C., Wuepper, D., Montanarella, L., Ballabio, C., 2020. Land use and climate change impacts on global soil erosion by water (2015–2070). *Proc. Natl. Acad. Sci.* 117 (36), 21994–22001. <https://doi.org/10.1073/pnas.2001403117>.
- BoSCO, C., RuSCO, E., MoNTANARELLA, L., PANAGoS, P., 2009. Soil erosion in the Alpine area: risk assessment and climate change. *Studi Trentini di scienze naturali* 85, 117–123.
- Calanca, P., 2007. Climate change and drought occurrence in the Alpine region: how severe are becoming the extremes? *Glob. Planet Change* 57 (1), 151–160. <https://doi.org/10.1016/j.gloplacha.2006.11.001>.
- Calvin, K., Patel, P., Clarke, L., Asrar, G., Bond-Lamberty, B., Cui, R.Y., Di Vittorio, A., Dorheim, K., Edmonds, J., Hartin, C., Hejazi, M., Horowitz, R., Iyer, G., Kyle, P., Kim, S., Link, R., McJeon, H., Smith, S.J., Snyder, A., Wise, M., 2019. GCAM v5.1: representing the linkages between energy, water, land, climate, and economic systems. *Geosci. Model Develop.* 12 (2), 677–698. <https://doi.org/10.5194/gmd-12-677-2019>.
- Carlson, B.Z., Corona, M.C., Dentant, C., Bonet, R., Thuiller, W., Choler, P., 2017. Observed long-term greening of alpine vegetation—A case study in the French Alps. *Environ. Res. Letters* 12 (11), 114006. <https://doi.org/10.1088/1748-9326/aa84bd>.
- Carr, T.W., Balković, J., Dodds, P.E., Folberth, C., Fulajtar, E., Skalsky, R., 2020. *Uncertainties, Sensitivities and Robustness of Simulated Water Erosion in an EPIC-based Global-Gridded Crop Model* [Preprint]. Earth System Science/Response to Global Change: Models, Holocene/Anthropocene. <https://doi.org/10.5194/bg-2020-93>.
- Chen, M., Vernon, C., 2020. *GCAM-Demeter LU Dataset* (No. Project ID: 68344; Instrument ID: 85000; Upload ID: 1188). Pacific Northwest National Laboratory 2; Pacific Northwest National Lab. (PNNL), Richland, WA (United States). <https://doi.org/10.25584/data.2020-04.1188/1614678>.
- Chen, M., Vernon, C.R., Graham, N.T., Hejazi, M., Huang, M., Cheng, Y., Calvin, K., 2020. Global land use for 2015–2100 at 0.05° resolution under diverse socioeconomic and climate scenarios. *Sci. Data* 7 (1). <https://doi.org/10.1038/s41597-020-00669-x>. Article 1.
- Chhetri, N., Stuhlmacher, M., Ishtiaque, A., 2019. Nested pathways to adaptation. *Environ. Res. Commun.* 1 (1), 015001. <https://doi.org/10.1088/2515-7620/aaf9f9>.
- Costanza, J.K., Terando, A.J., 2019. Landscape connectivity planning for adaptation to future climate and land-use change. *Curr. Landsc. Ecol. Rep.* 4 (1), 1–13. <https://doi.org/10.1007/s40823-019-0035-2>.
- Dessai, S., Hulme, M., 2004. Does climate adaptation policy need probabilities? *Clim. Policy* 22. <https://doi.org/10.1080/14693062.2004.9685515>.
- Díaz, S., Settele, J., Brondízio, E.S., Ngo, H.T., Agard, J., Armeth, A., Balvanera, P., Brauman, K.A., Butchart, S.H.M., Chan, K.M.A., Garibaldi, L.A., Ichii, K., Liu, J., Subramanian, S.M., Midgley, G.F., Miloslavich, P., Molnár, Z., Obura, D., Pfaff, A., ... Zayas, C.N. (2019). *Pervasive human-driven decline of life on Earth points to the need for transformative change*. 32. [10.1126/science.aax3100](https://doi.org/10.1126/science.aax3100).
- Duguma, L., Minang, P., Van Noordwijk, M., 2014. Climate Change mitigation and adaptation in the land use sector: from complementarity to synergy. *Environ. Manage.* 54. <https://doi.org/10.1007/s00267-014-0331-x>.
- Egarter Vigl, L., Tasser, E., Schirpke, U., Tappeiner, U., 2017. Using land use/land cover trajectories to uncover ecosystem service patterns across the Alps. *Reg. Environ. Change* 17 (8), 2237–2250. <https://doi.org/10.1007/s10113-017-1132-6>.
- Estrada-Carmona, N., Harper, E.B., DeClerck, F., Fremier, A.K., 2017. Quantifying model uncertainty to improve watershed-level ecosystem service quantification: a global sensitivity analysis of the RUSLE. *Int. J. Biodivers. Sci., Ecosyst. Serv. Manage.* 13 (1), 40–50. <https://doi.org/10.1080/21513732.2016.1237383>.
- Fedele, G., Locatelli, B., Djoudi, H., Colloff, M.J., 2018. Reducing risks by transforming landscapes: cross-scale effects of land-use changes on ecosystem services. *PLoS One* 13 (4), e0195895. <https://doi.org/10.1371/journal.pone.0195895>.
- Fu, B.J., Zhao, W.W., Chen, L.D., Zhang, Q.J., Lü, Y.H., Gulinck, H., Poesen, J., 2005. Assessment of soil erosion at large watershed scale using RUSLE and GIS: a case study in the Loess Plateau of China: ASSESSMENT OF SOIL EROSION USING RUSLE AND GIS. *Land Degrad. Develop.* 16 (1), 73–85. <https://doi.org/10.1002/ldr.646>.
- Gianinetto, M., Aiello, M., Vezzoli, R., Polinelli, F.N., Rulli, M.C., Chiarelli, D.D., Bocchiola, D., Ravazzani, G., Soncini, A., 2020. Future scenarios of soil erosion in the Alps under climate change and land cover transformations simulated with automatic machine learning. *Clim.* 8 (2), 28. <https://doi.org/10.3390/cli8020028>.
- Guerra, C.A., Maes, J., Geijzendorffer, I., Metzger, M.J., 2016. An assessment of soil erosion prevention by vegetation in Mediterranean Europe: current trends of ecosystem service provision. *Ecol. Indic.* 60, 213–222. <https://doi.org/10.1016/j.ecolind.2015.06.043>.
- Hamel, P., Bryant, B.P., 2017. Uncertainty assessment in ecosystem services analyses: seven challenges and practical responses. *Ecosyst. Serv.* 24, 1–15. <https://doi.org/10.1016/j.ecoser.2016.12.008>.
- Heltberg, R., Siegel, P.B., & Jorgensen, S.L. (2009). *Addressing Human vulnerability to climate change: toward a 'No regrets' Approach*.
- Hijmans, R.J., Eten, J.van, Sumner, M., Cheng, J., Baston, D., Bevan, A., Bivand, R., Bussetto, L., Canty, M., Fasoli, B., Forrest, D., Ghosh, A., Golicher, D., Gray, J., Greenberg, J.A., Hiemstra, P., Hingee, K., Ilich, A., Geosciences, I.for M.A., ... Wueest, R. (2022). *raster: geographic Data Analysis and Modeling* (Version 3.5-15) [Logiciel]. <https://CRAN.R-project.org/package=raster>.
- Hock, R., Rasul, G., Adler, C., Caceres, B., Gruber, S., Hirabayashi, Y., Jackson, M., Kääb, A., Kang, S., & Kutuzov, S. (2019). *High mountain areas: in: IPCC Special report on the Ocean and cryosphere in a changing climate*.
- Jones, H.P., Hole, D.G., Zavaleta, E.S., 2012. Harnessing nature to help people adapt to climate change. *Nat. Clim. Change* 2 (7), 504. <https://doi.org/10.1038/nclimate1463>.
- Kouli, M., Soupis, P., Vallianatos, F., 2009. Soil erosion prediction using the Revised Universal Soil Loss Equation (RUSLE) in a GIS framework, Chania, Northwestern Crete, Greece. *Environ. Geol.* 57 (3), 483–497. <https://doi.org/10.1007/s00254-008-1318-9>.
- Kumar, P., Debele, S.E., Sahani, J., Rawat, N., Marti-Cardona, B., Alfieri, S.M., Basu, B., Basu, A.S., Bowyer, P., Charizopoulos, N., Gallotti, G., Jaakko, J., Leo, L.S., Loupis, M., Menenti, M., Mickovski, S.B., Mun, S.-J., Gonzalez-Ollauri, A., Pfeiffer, J., Zieher, T., 2021. Nature-based solutions efficiency evaluation against natural hazards: modelling methods, advantages and limitations. *Sci. Total Environ.* 784, 147058. <https://doi.org/10.1016/j.scitotenv.2021.147058>.
- Lavorel, S., 2019. Climate change effects on grassland ecosystem services. D. J. Gibson & J. A. Newman (Eds.). *Grasslands and Climate Change*. Cambridge University Press, pp. 131–146. <https://doi.org/10.1017/9781108163941.010>, 1st éd.
- Lavorel, S., Colloff, M.J., Locatelli, B., Gordard, R., Prober, S.M., Gabillet, M., Devaux, C., Laforge, D., Peyrache-Gadeau, V., 2019. Mustering the power of ecosystems for adaptation to climate change. *Environ. Sci. Policy* 92, 87–97. <https://doi.org/10.1016/j.envsci.2018.11.010>.
- Lavorel, S., Locatelli, B., Colloff, M.J., Bruley, E., 2020. Co-producing ecosystem services for adapting to climate change. *Philosoph. Trans. R. Soc. B* 375 (1794), 20190119. <https://doi.org/10.1098/rstb.2019.0119>.
- López-Vicente, M., Navas, A., 2010. Routing runoff and soil particles in a distributed model with GIS: implications for soil protection in mountain agricultural landscapes. *Land Degrad. Develop.* 21 (2), 100–109. <https://doi.org/10.1002/ldr.901>.
- Lu, D., Li, G., Valladares, G.S., Batistella, M., 2004. Mapping soil erosion risk in Rondônia, Brazilian Amazonia: using RUSLE, remote sensing and GIS. *Land Degrad. Develop.* 15 (5), 499–512. <https://doi.org/10.1002/ldr.634>.
- Masson-Delmotte, V., Zhai, P., Pirani, A., Connors, S., Péan, C., Berger, S., Caud, N., Chen, Y., Goldfarb, L., Gomis, M., 2021. *IPCC 2021: Climate Change 2021: The Physical Science Basis: Contribution of Working Group I to the Sixth Assessment Report of the Intergovernmental Panel On Climate Change*. Cambridge University Press, Cambridge, UK.
- Mullan, D., Favis-Mortlock, D., Fealy, R., 2012. Addressing key limitations associated with modelling soil erosion under the impacts of future climate change. *Agric. For. Meteorol.* 156, 18–30. <https://doi.org/10.1016/j.agrformet.2011.12.004>.
- O'Neill, B.C., Krieglger, E., Riahi, K., Ebi, K.L., Hallegatte, S., Carter, T.R., Mathur, R., van Vuuren, D.P., 2014. A new scenario framework for climate change research: the concept of shared socioeconomic pathways. *Clim. Change* 122 (3), 387–400. <https://doi.org/10.1007/s10584-013-0905-2>.
- Panagos, P., Ballabio, C., Borrelli, P., Meusburger, K., Klik, A., Rouseva, S., Tadić, M.P., Michaelides, S., Hrabalíková, M., Olsen, P., Aalto, J., Lakatos, M., Rymaszewicz, A., Dumitrescu, A., Beguería, S., Alewell, C., 2015. Rainfall erosivity in Europe. *Sci. Total Environ.* 511, 801–814. <https://doi.org/10.1016/j.scitotenv.2015.01.008>.
- Panagos, P., Ballabio, C., Himics, M., Scarpa, S., Matthews, F., Bogonos, M., Poesen, J., Borrelli, P., 2021. Projections of soil loss by water erosion in Europe by 2050. *Environ. Sci. Policy* 124, 380–392. <https://doi.org/10.1016/j.envsci.2021.07.012>.
- Panagos, P., Borrelli, P., Poesen, J., Ballabio, C., Lugato, E., Meusburger, K., Montanarella, L., Alewell, C., 2015c. The new assessment of soil loss by water erosion in Europe. *Environ. Sci. Policy* 54, 438–447. <https://doi.org/10.1016/j.envsci.2015.08.012>.
- Pyke, C.R., Andelman, S.J., 2007. Land use and land cover tools for climate adaptation. *Clim. Change* 80 (3), 239–251. <https://doi.org/10.1007/s10584-006-9110-x>.
- R Core Team, 2018. *R: A Language and Environment for Statistical Computing*. R Foundation for Statistical Computing. <https://www.R-project.org/>.
- Refsgaard, J.C., van der Sluijs, J.P., Højberg, A.L., Vanrolleghem, P.A., 2007. Uncertainty in the environmental modelling process – A framework and guidance. *Environ. Modell. Softw.* 22 (11), 1543–1556. <https://doi.org/10.1016/j.envsoft.2007.02.004>.
- Renard, K.G. (1997). *Predicting soil erosion by water: a guide to conservation planning with the revised universal soil loss equation (RUSLE)* (K. G. Renard, USA, & USA, Eds.).
- Renard, K.G., Freimund, J.R., 1994. Using monthly precipitation data to estimate the R-factor in the revised USLE. *J. Hydrol.* 157 (1–4), 287–306. [https://doi.org/10.1016/0022-1694\(94\)90110-4](https://doi.org/10.1016/0022-1694(94)90110-4).
- Rey, F., 2021. Harmonizing erosion control and flood prevention with restoration of biodiversity through ecological engineering used for Co-benefits nature-based solutions. *Sustainability* 13 (20), 11150. <https://doi.org/10.3390/su132011150>.
- Riahi, K., van Vuuren, D.P., Krieglger, E., Edmonds, J., O'Neill, B.C., Fujimori, S., Bauer, N., Calvin, K., Dellink, R., Fricko, O., Lutz, W., Popp, A., Cuarema, J.C., Kc, S., Leimbach, M., Jiang, L., Kram, T., Rao, S., Emmerling, J., Tavoni, M., 2017. The Shared Socioeconomic Pathways and their energy, land use, and greenhouse gas emissions implications: an overview. *Global Environ. Change* 42, 153–168. <https://doi.org/10.1016/j.gloenvcha.2016.05.009>.

- Schägnler, J.P., Brander, L., Maes, J., Hartje, V., 2013. Mapping ecosystem services' values : current practice and future prospects. *Ecosyst. Serv.* 4, 33–46. <https://doi.org/10.1016/j.ecoser.2013.02.003>.
- Schirpke, U., Kohler, M., Leitinger, G., Fontana, V., Tasser, E., Tappeiner, U., 2017. Future impacts of changing land-use and climate on ecosystem services of mountain grassland and their resilience. *Ecosyst. Serv.* 26, 79–94. <https://doi.org/10.1016/j.ecoser.2017.06.008>.
- Siders, A., Pierce, A.L., 2021. Deciding how to make climate change adaptation decisions. *Curr. Opin. Environ. Sustain.* 52, 1–8. <https://doi.org/10.1016/j.cosust.2021.03.017>.
- Soini, K., Anderson, C.C., Polderman, A., Teresa, C., Sisay, D., Kumar, P., Mannocchi, M., Mickovski, S., Panga, D., Pilla, F., Preuschmann, S., Sahani, J., Tuomenvirta, H., 2023. Context matters : co-creating nature-based solutions in rural living labs. *Land use policy.* 133, 106839. <https://doi.org/10.1016/j.landusepol.2023.106839>.
- Song, X.-P., Hansen, M.C., Stehman, S.V., Potapov, P.V., Tyukavina, A., Vermote, E.F., Townshend, J.R., 2018. Global land change from 1982 to 2016. *Nature* 560 (7720), 639–643. <https://doi.org/10.1038/s41586-018-0411-9>.
- Sørland, S.L., Schär, C., Lüthi, D., Kjellström, E., 2018. Bias patterns and climate change signals in GCM-RCM model chains. *Environ. Res. Lett.* 13 (7), 074017. <https://doi.org/10.1088/1748-9326/aacc77>.
- Stritih, A., Bebi, P., Grêt-Regamey, A., 2018. Quantifying uncertainties in earth observation-based ecosystem service assessments. *Environ. Modell. Softw.* <https://doi.org/10.1016/j.envsoft.2018.09.005>.
- van Vliet, M.T.H., van Beek, L.P.H., Eisner, S., Flörke, M., Wada, Y., Bierkens, M.F.P., 2016. Multi-model assessment of global hydropower and cooling water discharge potential under climate change. *Global Environ. Change* 40, 156–170. <https://doi.org/10.1016/j.gloenvcha.2016.07.007>.
- van Vuuren, D.P., Edmonds, J., Kainuma, M., Riahi, K., Thomson, A., Hibbard, K., Hurtt, G.C., Kram, T., Krey, V., Lamarque, J.-F., Masui, T., Meinshausen, M., Nakicenovic, N., Smith, S.J., Rose, S.K., 2011. The representative concentration pathways : an overview. *Clim. Change* 109 (1), 5. <https://doi.org/10.1007/s10584-011-0148-z>.
- Vanwalleghem, T., Gómez, J.A., Infante Amate, J., González de Molina, M., Vanderlinden, K., Guzmán, G., Laguna, A., Giráldez, J.V., 2017. Impact of historical land use and soil management change on soil erosion and agricultural sustainability during the Anthropocene. *Anthropocene* 17, 13–29. <https://doi.org/10.1016/j.ancene.2017.01.002>.
- Veerkamp, C.J., Loreti, M., Benavidez, R., Jackson, B., Schipper, A.M., 2023. Comparing three spatial modeling tools for assessing urban ecosystem services. *Ecosyst. Serv.* 59, 101500. <https://doi.org/10.1016/j.ecoser.2022.101500>.
- Verfaillie, D., Déqué, M., Morin, S., Lafaysse, M., 2017. The method ADAMONT v1.0 for statistical adjustment of climate projections applicable to energy balance land surface models. *Geosci. Model Develop.* 10 (11), 4257–4283. <https://doi.org/10.5194/gmd-10-4257-2017>.
- Vetter, T., Huang, S., Aich, V., Yang, T., Wang, X., Krysanova, V., Hattermann, F., 2015. Multi-model climate impact assessment and intercomparison for three large-scale river basins on three continents. *Earth Syst. Dyn.* 6 (1), 17–43. <https://doi.org/10.5194/esd-6-17-2015>.
- Visser, H., Petersen, A.C., Beusen, A.H.W., Heuberger, P.S.C., Janssen, P.H.M., 2006. *Guidance for uncertainty assessment and communication. Report 550032001, 2006.*
- Walker, W.E., Harremoës, P., Rotmans, J., van der Sluijs, J.P., van Asselt, M.B.A., Janssen, P., Kraayer von Krauss, M.P., 2003. Defining uncertainty : a conceptual basis for uncertainty management in model-based decision support. *Integr. Assess.* 4 (1), 5–17. <https://doi.org/10.1076/iaij.4.1.5.16466>.
- Wang, Z., Lechner, A.M., Baumgartl, T., 2018. Ecosystem services mapping uncertainty Assessment : a case study in the Fitzroy Basin mining region. *Water. (Basel)* 10 (1). <https://doi.org/10.3390/w10010088>. Article 1.
- Wischmeier, W.H., Smith, D.D., 1978. *Predicting rainfall erosion losses. Agricultural Handbook 537. Agricultural Research Service, United States Department of Agriculture.*
- Zhang, H., Yang, Q., Li, R., Liu, Q., Moore, D., He, P., Ritsema, C.J., Geissen, V., 2013. Extension of a GIS procedure for calculating the RUSLE equation LS factor. *Comput. Geosci.* 52, 177–188. <https://doi.org/10.1016/j.cageo.2012.09.027>.